Regular Article

blood

MYELOID NEOPLASIA

Heterogeneous resistance to quizartinib in acute myeloid leukemia revealed by single-cell analysis

Catherine C. Smith,[1,2] Amy Paguirigan,[3] Grace R. Jeschke,[4] Kimberly C. Lin,[1] Evan Massi,[1] Theodore Tarver,[1] Chen-Shan Chin,[5] Saurabh Asthana,[2] Adam Olshen,[2,6] Kevin J. Travers,[5] Susana Wang,[5] Mark J. Levis,[7] Alexander E. Perl,[4] Jerald P. Radich,[3] and Neil P. Shah[1,2]

[1]Division of Hematology/Oncology and [2]Helen Diller Family Comprehensive Cancer Center, University of California, San Francisco, San Francisco, CA; [3]Fred Hutchinson Cancer Research Center, Seattle, WA; [4]Division of Hematology/Oncology, Abramson Cancer Center, University of Pennsylvania, Philadelphia, PA; [5]Pacific Biosciences, Menlo Park, CA; [6]Department of Epidemiology and Biostatistics, University of California, San Francisco, San Francisco, CA; and [7]Department of Oncology, Sidney Kimmel Comprehensive Cancer Center, Johns Hopkins University, Baltimore, MD

Key Points

- Polyclonal mechanisms of resistance, demonstrated by single-cell analysis, occur in the majority of AML patients who relapse on quizartinib.

Genomic studies have revealed significant branching heterogeneity in cancer. Studies of resistance to tyrosine kinase inhibitor therapy have not fully reflected this heterogeneity because resistance in individual patients has been ascribed to largely mutually exclusive on-target or off-target mechanisms in which tumors either retain dependency on the target oncogene or subvert it through a parallel pathway. Using targeted sequencing from single cells and colonies from patient samples, we demonstrate tremendous clonal diversity in the majority of acute myeloid leukemia (AML) patients with activating *FLT3* internal tandem duplication mutations at the time of acquired resistance to the FLT3 inhibitor quizartinib. These findings establish that clinical resistance to quizartinib is highly complex and reflects the underlying clonal heterogeneity of AML. (*Blood*. 2017;130(1):48-58)

Introduction

Acute myeloid leukemia (AML) is an aggressive hematopoietic malignancy historically categorized into defined genetic subgroups by cytogenetic studies that can be used to predict prognosis and direct clinical decision-making. Recent large-scale genomic sequencing efforts demonstrate that AML is among the least genetically complex of all extensively sequenced human malignancies; a small number of genes are recurrently mutated in de novo AML, and the average number of genetic events in a given leukemic sample is low.[1,2] Despite this, multiple groups have demonstrated the clonal heterogeneity of AML and advocated a model of disease in which the collective accumulation of genetic events in hematopoietic stem cells (HPSCs) facilitates stepwise tumor evolution from preleukemic to leukemic stem cells.[3-7] Frequently, the accrual of genetic events drives the clonal evolution of secondary AML from antecedent myelodysplastic syndrome in which multiple AML subclones arise in a linear fashion and at disease relapse in which divergent clones can emerge after chemotherapy.[6,8] Functionally, heterogeneous AML subclones identified in an individual patient can display distinct cellular phenotypes and functional properties.[9]

Constitutively activating mutations in FMS-like tyrosine kinase 3 (*FLT3*) that comprise internal tandem duplication (ITD) mutations in the juxtamembrane domain or point mutations in the tyrosine kinase domain (KD) are frequently acquired late in AML tumor evolution.[4,6] Nonetheless, quizartinib (AC220), a highly selective investigational tyrosine kinase inhibitor (TKI) of FLT3-ITD, has demonstrated an impressive composite complete remission rate of approximately 50% in relapsed or refractory AML patients with *FLT3*-ITD mutations.[10-12] Although responses to quizartinib are largely short-lived, relapses to date have been exclusively associated with acquired on-target resistance mutations in the *FLT3*-ITD KD, demonstrating continued tumor reliance on mutant FLT3 activity. We reported new resistance-conferring secondary mutations at the activation loop residue D835 or the gatekeeper residue F691in the KD of *FLT3*-ITD in 8 of 8 patients who relapsed after achieving clearance of bone marrow blasts on quizartinib therapy.[13] Other groups have found similar results in the case of acquired resistance to quizartinib[14] and to the multikinase inhibitor sorafenib,[15,16] which also has single-agent activity in *FLT3*-ITD$^+$ AML.[17] Several patients developed more than 1 KD mutation in *FLT3*-ITD at the time of relapse,[13] revealing the presence of tumor heterogeneity in FLT3 inhibitor-resistant disease. Notably, in all patients analyzed in this study, the drug-resistant KD mutation was found in only ~20% to 50% of *FLT3*-ITD$^+$ alleles, raising the possibility of competing mechanisms of non-FLT3–dependent resistance. Reactivation of parallel or downstream signaling pathways in clinical resistance has been observed with inhibitors of BTK in chronic lymphocytic leukemia,[18] BRAF in melanoma,[19-21] and EGFR in non–small cell lung cancer.[22] However, the extent to which off-target mechanisms account for FLT3 inhibitor resistance in patients remains unknown.

The experimental elucidation of tumor heterogeneity in clinical isolates can be technically difficult. By using bulk sequencing methods, clonal composition of tumor populations can be computationally

Submitted 21 April 2016; accepted 3 May 2017. Prepublished online as *Blood* First Edition paper, 10 May 2017; DOI 10.1182/blood-2016-04-711820.

The online version of this article contains a data supplement.

The publication costs of this article were defrayed in part by page charge payment. Therefore, and solely to indicate this fact, this article is hereby marked "advertisement" in accordance with 18 USC section 1734.

estimated from mutant allele frequencies; however, as we recently described, single-cell analysis can uncover clonal diversity in AML that cannot be fully illuminated by computational methods.[7] In recognition of clonal heterogeneity in AML and off-target TKI resistance mechanisms described in other malignancies, we sought to examine (via single-cell and colony genotyping) the extent to which clinical resistance to quizartinib is polyclonal in nature and comprises on- and off-target mechanisms.

Methods

Patient samples

Samples were obtained from patients enrolled on phase 2 clinical trials of quizartinib in relapsed or refractory AML at the University of California-San Francisco, University of Pennsylvania, or Johns Hopkins University according to the Declaration of Helsinki using institutional review board–approved protocols. Details of the clinical trials and results are reported elsewhere.[10-12]

FLT3 KD analysis by polymerase chain reaction subcloning and single-molecule real-time sequencing

Details of amplification of the *FLT3* KD, polymerase chain reaction (PCR) subcloning, single-molecule real-time sequencing sample preparation, and sequencing analysis were as previously described.[13]

Cell lines

Stable Ba/F3 lines were generated by retroviral infection with the appropriate mutated plasmid as previously described.[13]

Cell viability assay

Exponentially growing cells (5×10^3 cells per well) were plated in each well of a 96-well plate with 0.1 mL of RPMI 1640 plus 10% fetal calf serum containing the appropriate concentration of quizartinib (Selleckchem, Houston, TX) in triplicate, and cell viability was assessed after 48 hours as previously described.[23] Numerical 50% inhibitory dose (IC_{50}) values were generated by using nonlinear best-fit regression analysis with Prism 5 software (GraphPad, San Diego, CA), and reported values are the average of 3 or more experiments.

Immunoblotting

Exponentially growing Ba/F3 cells stably expressing mutant isoforms were plated in RPMI 1640 medium plus 10% fetal calf serum supplemented with quizartinib at the indicated concentration. After a 90-minute incubation, the cells were washed in phosphate-buffered saline and lysed and processed as previously described.[13,23] Immunoblotting was performed by using anti-phospho-FLT3, anti-phospho-STAT5, anti-STAT5, anti-phospho-ERK, anti-ERK, anti-phospho-S6, anti-S6 (Cell Signaling, Beverly, MA), and anti-FLT3 S18 antibody (Santa Cruz Biotechnology, Santa Cruz, CA). Data shown are representative of multiple experiments.

Single cell sorting and genotyping

Cryogenically stored patient samples were defrosted, stained with calcein violet (Life Technologies) to select viable cells for single-cell sorting in 384-well PCR plates as previously described.[7] Cells were sorted dry and frozen to store until PCR was performed. PCR reactions were performed by adding 10 μL of PCR mix to each well containing cells, empty wells (as controls), and those containing reference DNA from both cell lines and the specific patients per plate. A single 10-μL duplex PCR reaction was performed with the following primer sets: *FLT3*-ITD forward 5′-CTTTCCTCTATCTGCAGAACTGCCT-3′ and reverse 5′-GCATGGGTGGGAAACTGTGCCT-3′, each at 100 nM, and *FLT3*-D835 forward 5′- CTCACGGCACAGCCCAGTAAAGA-3′ and reverse 5′-TTGCACTCAAAGGCCCCTAACTGAT-3′, each at 200 nM. Nested PCR reactions were then performed on the product to detect *FLT3*-ITD via a fragment analysis assay that used a fluorescently labeled forward primer (5′-FAM-AGCAATTTAGGTATGAAAGCCAGC-3′) and an unlabeled reverse primer (5′-CTTTCAGCATTTTGACGGCAACC-3′) (each at 200 nM) or to detect the *FLT3*-D835 sequence via pyrosequencing using an unlabeled forward primer (5′- AGGAACGTGCTTGTCACCC-3′) and a biotinylated reverse primer (5′- GCCCCTGACAACATAGTTGGA-3′) (each at 250 nM) with a pyrosequencing primer (5′- GATATGTGACTTTGGATTG-3′). The results of these 2 genotyping assays were then manually scored by using empirically determined thresholds for both assays as performed previously or according to the manufacturer's suggestions (QIAGEN, for pyrosequencing). The resulting genotypes were then combined and data were reported. Assays were validated as previously described before use on patient samples.[7]

Colony assays in primary patient blasts

Clonogenic assays were performed as previously described.[24] To sequence colonies, they were plucked in volumes <2 μL and frozen. Colonies were then thawed, 2 to 5 μL of molecular biology grade water was added, and the colonies were incubated at 95°C for 5 minutes before being put on ice. A single 25-μL duplex PCR reaction was performed on the resulting lysate, with the primer sets described above at the same concentrations. Nested reactions were then performed on the product to detect *FLT3*-ITD via a fragment analysis assay using matched primer sets as described above. The results of these 2 genotyping assays were then manually scored by using empirically determined thresholds for both assays as performed previously or according to the manufacturer's suggestions (QIAGEN, for pyrosequencing). The resulting genotypes were then combined, and data were reported.

Targeted exome sequencing

Targeted next-generation sequencing of 33 genes (supplemental Table 7, available on the *Blood* Web site) associated with hematologic malignancies was conducted by the Center for Personalized Diagnostics at the University of Pennsylvania as previously described.[25] Average read depth was 3000X, minimal depth was 250X, and reporting frequency cutoff for variants was 5%, except for *FLT3*-ITD for which the variant detection cutoff was 1%. Mutations were classified into 4 categories: pathogenic, likely disease-associated, variant of uncertain significance, or likely benign on the basis of a review of publically available data; only pathogenic or likely disease-associated mutations were included in this analysis.

Whole-exome sequencing

Paired pretreatment and relapse samples from patients 1005-007, 1009-003, and 3351-1085 were prepared for exome capture with the SureSelect 50 Mb All Exon kit (Agilent Technologies) following standard protocols. Paired-end sequencing (2×100 bp) was performed by using HiSeq2000 sequencing instruments at Centrillion Biosciences (Palo Alto, CA). Illumina HiSeq analysis produced between 105.6 and 119.6 million paired-end reads per sample at 107-126X depth (supplemental Table 10). Reads were aligned against human genome (National Center for Biotechnology Information build GRCh37/hg19) with Burrows-Wheeler Aligner,[26] followed by base quality score recalibration and local indel realignment with the Genome Analysis Toolkit[27] and deduplication with Picard tools. Subsequently, somatic mutations unique to the relapse sample were called by using MuTect[28] and compared with the pretreatment sample. Mutations were further filtered to exclude mutant reads in the pretreatment sample, and they required at least 4 mutant reads in the relapse sample.

Results

Heterogeneity of *FLT3* D835 mutations in clinical resistance to quizartinib

Given the established importance of *FLT3* KD mutations in clinical resistance to quizartinib, we first focused on determining the diversity of drug-resistant mutant alleles within *FLT3* itself. By using an in vitro

Table 1. Percentage of D835 mutations in ITD$^+$ and native *FLT3* (ITD$^-$) alleles in complementary DNA from patients who relapse on quizartinib

Patient number	Sequences ITD$^{+/-}$	Mutation	No. of ITD$^{+/-}$ sequences sampled	Observed alternative codon frequency of ITD$^+$ or ITD$^-$ alleles (%)
1005-006	ITD$^+$	D835Y	261	39.50
	ITD$^+$	D835F	261	2.70
	ITD$^-$	D835Y	564	16.80
1005-007	ITD$^+$	D835V	378	47.40
	ITD$^+$	D835Y	378	4.00
	ITD$^-$	D835V	255	24.70
1005-009	ITD$^+$	D835Y	445	50.60
	ITD$^-$	D835Y	10	50.00
1009-003	ITD$^+$	D835F	322	10.60
	ITD$^+$	D835Y	322	8.70
	ITD$^+$	D835V	322	3.40
	ITD$^-$	D835Y	266	7.50
	ITD$^-$	D835F	266	3.80
1009-007	ITD$^+$	D835Y	235	55.70
	ITD$^-$	D835Y	393	25.20
1011-006	ITD$^+$	D835Y	402	41.00
	ITD$^-$	D835Y	825	9.20
1011-007	ITD$^+$	D835V	436	29.60
	ITD$^+$	D835Y	436	3.00
	ITD$^-$	D835V	64	28.10

mutagenesis screen, we previously demonstrated that several substitutions at the *FLT3* D835 residue confer resistance to quizartinib when found in cis (on the same allele) with an activating ITD mutation.[13] Consequently, we focused our original analysis on ITD-containing alleles of patients who relapsed on quizartinib and initially identified evolution of quizartinib-resistant KD mutations on the *FLT3*-ITD allele in 8 of 8 patients who achieved clearance of bone marrow blasts to ≤5% on quizartinib, including 6 patients with mutations at the D835 residue.[13] Four of these 8 had evidence of polyclonal resistance as evidenced by more than 1 detectable resistant KD mutation at relapse. Given that D835 mutations in native *FLT3* (ie, in the absence of an ITD) are constitutively activating and known to occur de novo in AML patients,[29] we then sought to assess whether such D835 mutations were detectable on the native *FLT3* allele of patients who relapsed on quizartinib. Surprisingly, we identified D835V, Y, and F mutations on the native *FLT3* allele in all 7 patients who had developed D835 codon substitutions on the ITD$^+$ allele at the time of relapse, including 1 patient (1009-007) not available at the time of our initial report[13] (Table 1). Curiously, the native *FLT3*-associated mutations identified represented a subset of the substitutions found on the ITD-containing allele in all cases. The proportion of native *FLT3* alleles containing D835 mutations ranged from 3.8% to 50% (Table 1). In 1 patient (1009-003) with D835V/Y/F mutations detected on ITD$^+$ alleles, both D835Y and D835F substitutions were observed on native *FLT3* alleles. When recreated in Ba/F3 cells, D835V/Y/F mutations in the context of native *FLT3* conferred substantial relative resistance to quizartinib in both proliferation and biochemical assays (Figure 1; supplemental Tables 1 and 2) when compared with *FLT3*-ITD, although to a lesser extent than D835 mutations found in cis with ITD (Figure 1; supplemental Table 2). With one exception (1005-009), D835 mutations in either ITD$^+$ or native *FLT3* alleles before quizartinib therapy were not detected (supplemental Table 3). Patient 1005-009 had low percentages (3.7% to 10.4%) of D835V/Y/F mutations on native *FLT3* alleles before quizartinib treatment, but at the time of overt clinical relapse, a homozygous ITD$^+$ clone was dominant, with 98% of alleles containing an ITD (supplemental Table 4) and 50% of the ITD$^+$ sequences harboring a D835Y mutation (Table 1). In light of the lesser relative resistance of D835 mutations when found on native *FLT3* alleles, this finding suggests that sufficient serum levels of quizartinib may effectively suppress these clones.

Polyclonal resistant blast populations exist in patients at relapse on quizartinib

In our previous work, we used a single-cell, multiplexed PCR-based assessment of mutations in *FLT3* and *NPM1* to reveal the presence of 5 to 15 genetically unique subpopulations in individual AML patient samples.[7] By using a similar approach, we performed single-cell sorting of viably frozen blasts from 3 patients (1005-007, 1005-009, 1009-003) with *FLT3-ITD* D835 mutations (but no other *FLT3* KD mutations) identified at the time of relapse, and we genotyped *FLT3* for both ITD and D835 mutations in single cells (Figure 2; supplemental Table 5). This analysis revealed striking genetic heterogeneity, with 8 to 18 cellular subpopulations identified per sample. In 2 of 3 patients, polyclonal D835 mutations were found in both ITD$^+$ and native *FLT3* cells (Figure 2; supplemental Table 5). The exception was a sample from patient 1005-009, which was previously noted to harbor a dominant homozygous ITD$^+$ clone (445 ITD$^+$ alleles vs 10 native *FLT3* alleles observed in a relapse sample; Table 1). In all patients, *FLT3*-ITD and D835 mutations were found in both heterozygous and homozygous combinations, although the distribution of zygosity of each mutation varied across samples. For example, patient 1005-009 demonstrated 2 different D835Y alleles resulting from distinct codon substitutions (GAT>TAT and GAT>TAC) found in combination with heterozygous or homozygous ITD alleles, whereas patient 1009-003 demonstrated 3 different D835 substitutions (V/Y/F) found in combination with heterozygous or homozygous ITD alleles along with 2 substitutions (D835Y/F) found without ITD. The allele frequencies of ITD and D835 mutations from single-cell genotyping was consistent with the allele frequencies observed by sequencing DNA extracted from the bulk cell populations (supplemental Table 4). The genomic DNA allele frequencies observed also approximated the allele frequencies observed in expressed alleles in complementary DNA derived from the bulk population (supplemental Table 4), suggesting

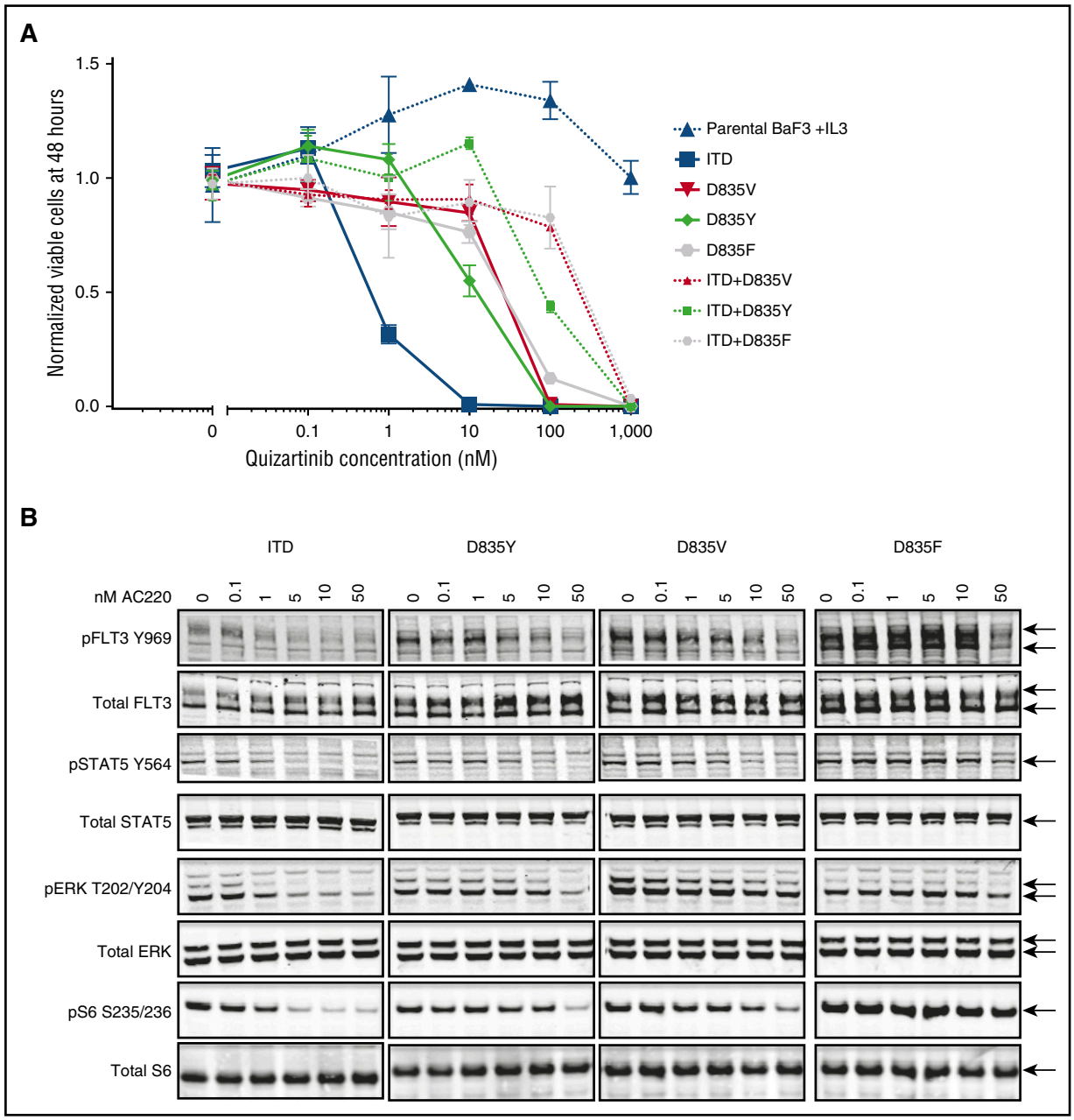

Figure 1. D835 mutations in native FLT3 cause resistance to quizartinib. (A) Normalized cell viability of Ba/F3 populations stably expressing FLT3-mutant isoforms after 48 hours in various concentrations of quizartinib (error bars represent standard deviation of triplicates from the same experiment). (B) Western blot analysis using the indicated antibodies performed on lysates from interleukin-3–independent Ba/F3 populations expressing the FLT3-mutant isoforms indicated. Cells were exposed to quizartinib at the noted concentrations for 90 minutes.

that FLT3 allele-specific overexpression at the RNA level does not play a significant role in quizartinib resistance. Although this single-cell genotyping technique cannot distinguish between *FLT3* ITD and D835 mutations occurring in cis or in trans (on different alleles), Ba/F3 cells expressing *FLT3* ITD and D835 mutations in trans demonstrated relative resistance to quizartinib similar to that demonstrated by cells expressing D835 mutations in native *FLT3* only (supplemental Figure 1) but less resistance than cells expressing *FLT3* ITD and D835 mutations in cis. Surprisingly, in all 3 patients, approximately 30% to 50% of *FLT3*-ITD$^+$ cells had no identifiable quizartinib-resistant *FLT3* D835 mutation, suggesting the presence of competing non-FLT3–dependent resistance mechanisms in these patients (Figure 2; supplemental Table 5).

FLT3-ITD$^+$ cells without *FLT3* D835 mutations are functionally resistant to quizartinib

To determine whether ITD$^+$ cells lacking *FLT3* D835 mutations observed in relapsed patient samples are representative of leukemic blasts that are functionally resistant to quizartinib (rather than terminally differentiated or nonproliferating cells), we analyzed blasts obtained at the time of relapse from a fourth patient (3351-1085) who initially achieved clearance of bone marrow blasts on quizartinib and developed a D835Y mutation (but no other KD mutations) at relapse. We performed a colony assay in the presence of 20 nM quizartinib. As expected, this concentration of quizartinib did not suppress the colony-forming ability of these blasts, thereby

A

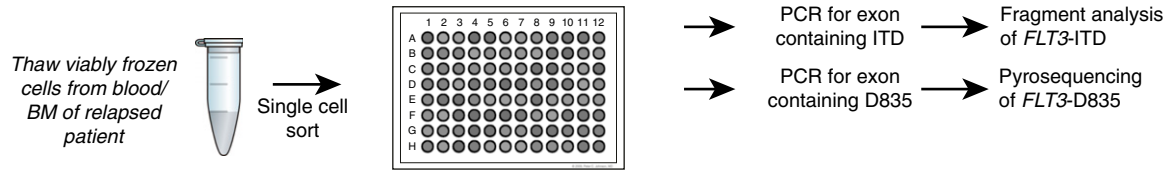

B

	FLT3-ITD zygosity	*FLT3*-D835 zygosity	*FLT3*-D835 mutation	% of total cells (310 cells total)
	Wild type	Wild type	--	11.3
	Wild type	Heterozygous	GTT (D835V)	2.2
	Wild type	Homozygous	GTT (D835V)	3.5
	Wild type	Heterozygous	TAT (D835Y)	0.6
	Heterozygous	Wild type	--	32.9
	Heterozygous	Heterozygous	GTT (D835V)	15.5
	Heterozygous	Homozygous	GTT (D835V)	16.1
	Heterozygous	Heterozygous	TAT (D835Y)	4.2
	Heterozygous	Homozygous	TAT (D835Y)	0.6
	Homozygous	Wild type	--	8.1
	Homozygous	Heterozygous	GTT (D835V)	1.9
	Homozygous	Homozygous	GTT (D835V)	2.6
	Homozygous	Heterozygous	TAT (D835Y)	0.3

1005-007

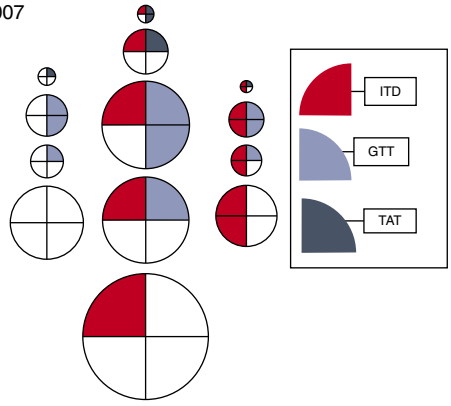

C

	FLT3-ITD zygosity	*FLT3*-D835 zygosity	*FLT3*-D835 mutation	% of total cells (188 cells total)
	Wild type	Wild type	--	6.3
	Heterozygous	Wild type	--	5.3
	Heterozygous	Heterozygous	TAT (D835Y)	1.0
	Heterozygous	Homozygous	TAT (D835Y)	2.7
	Heterozygous	Heterozygous	TAC (D835Y)	0.5
	Homozygous	Wild type	--	45.2
	Homozygous	Heterozygous	TAT (D835Y)	37.8
	Homozygous	Heterozygous	TAC (D835Y)	1.0

1005-009

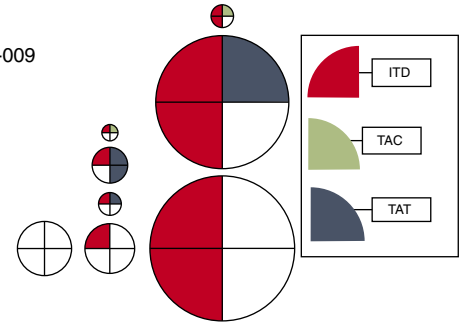

D

	FLT3-ITD zygosity	*FLT3*-D835 zygosity	*FLT3*-D835 mutation	% of total cells (271 cells total)
	Wild type	Wild type	--	18.9
	Wild type	Heterozygous	TAT (D835Y)	1.5
	Wild type	Homozygous	TAT (D835Y)	3.0
	Wild type	Heterozygous	TTT (D835F)	0.4
	Wild type	Homozygous	TTT (D835F)	1.1
	Heterozygous	Wild type	--	16.6
	Heterozygous	Heterozygous	TAT (D835Y)	10.7
	Heterozygous	Homozygous	TAT (D835Y)	2.2
	Heterozygous	Heterozygous	GTT (D835V)	4.8
	Heterozygous	Homozygous	GTT (D835V)	0.4
	Homozygous	Heterozygous	TTT (D835F)	9.2
	Homozygous	Homozygous	TTT (D835F)	3.0
	Homozygous	Wild type	--	14.0
	Homozygous	Heterozygous	TAT (D835Y)	5.5
	Homozygous	Homozygous	TAT (D835Y)	0.4
	Homozygous	Heterozygous	GTT (D835V)	1.1
	Homozygous	Heterozygous	TTT (D835F)	3.0
	Homozygous	Homozygous	TTT (D835F)	4.4

1009-003

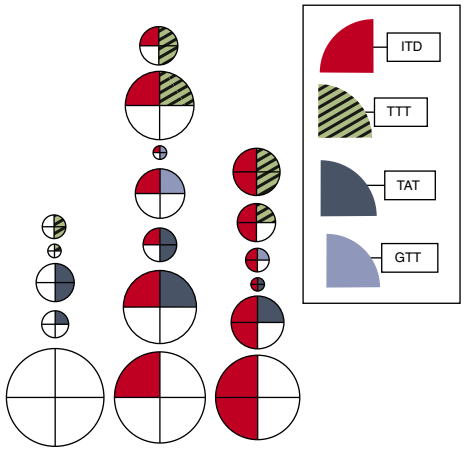

Figure 2.

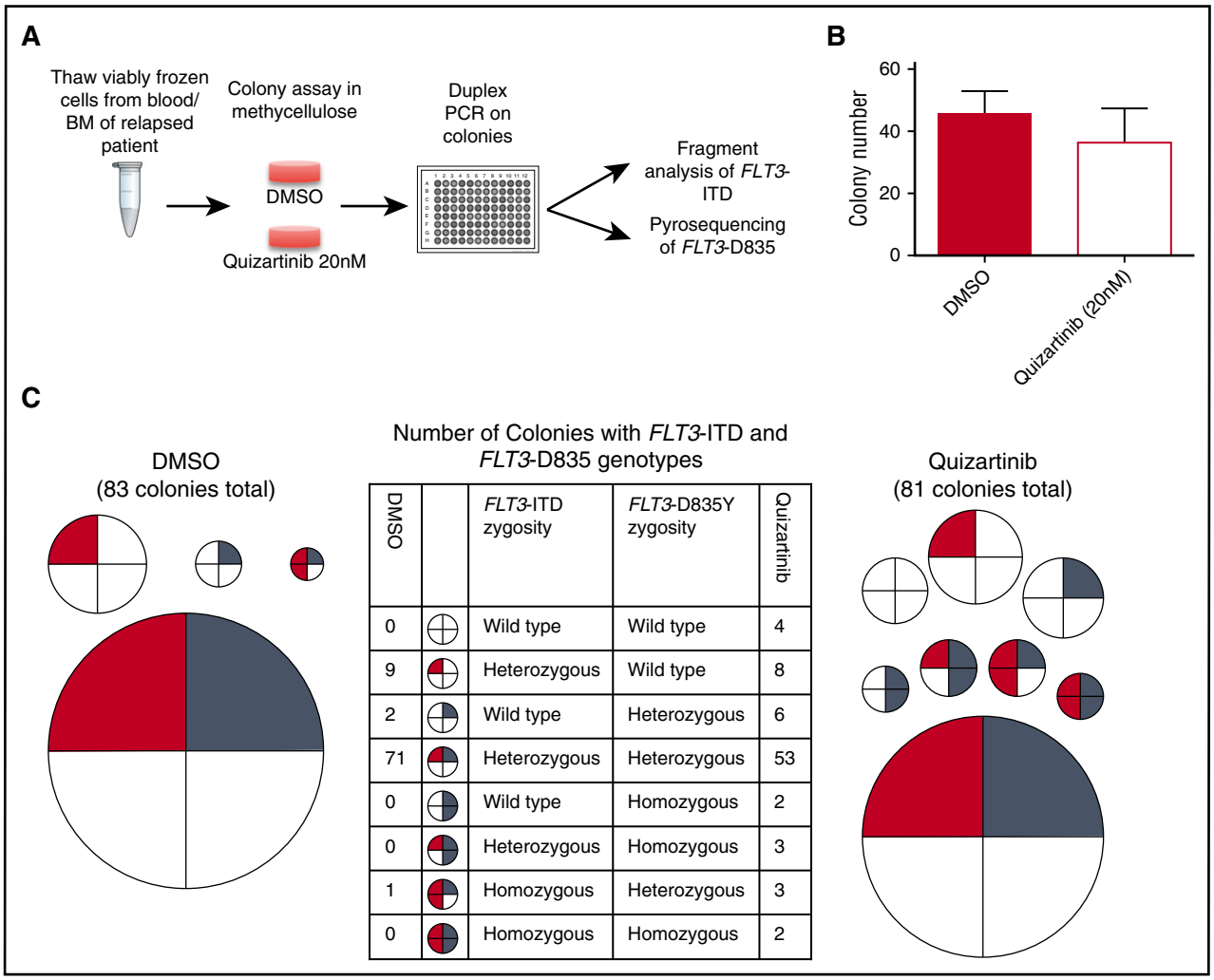

DMSO		FLT3-ITD zygosity	FLT3-D835Y zygosity	Quizartinib
0		Wild type	Wild type	4
9		Heterozygous	Wild type	8
2		Wild type	Heterozygous	6
71		Heterozygous	Heterozygous	53
0		Wild type	Homozygous	2
0		Heterozygous	Homozygous	3
1		Homozygous	Heterozygous	3
0		Homozygous	Homozygous	2

Figure 3. Genetic heterogeneity in colonies grown from a patient relapsed on quizartinib. (A) Schematic of experimental setup for genotyping of colonies grown from bone marrow of a patient relapsed after a response to quizartinib. (B) Number of colonies after 14 days in methylcellulose in dimethyl sulfoxide (DMSO) and 20 nM quizartinib. Error bars represent standard error of triplicate platings. (C) *FLT3* genotype of single colonies plucked from methylcellulose after 14 days of growth in DMSO or 20 nM quizartinib. Each circle represents a particular *FLT3* genotype. The relative size of circles is representative of the relative proportion of the overall population with that genotype. Number of colonies with each genotype is shown for DMSO (left) and quizartinib 20 nM (right).

confirming their resistance to quizartinib (Figure 3). Although a pretreatment cellular sample from this patient was not available for functional comparison, 20 nM quizartinib is sufficient to suppress colony formation of pretreatment samples from other *FLT3*-ITD$^-$ AML patients who achieved remission on quizartinib (supplemental Figure 2). Genotyping of individual colonies derived from this relapse sample in the presence of 20 nM quizartinib again showed striking genetic heterogeneity, including ITD$^+$ and native *FLT3* colonies with D835Y mutations in homozygous and heterozygous combinations as well as ITD$^+$ colonies without D835Y mutations (Figure 3; supplemental Table 6), again suggestive of non-*FLT3*–dependent resistance in a subset of blasts. In addition, 4 colonies with no *FLT3* alterations were identified in this sample, suggesting the presence of a quizartinib-resistant non-*FLT3*–mutant blast population, although we cannot exclude the possibility that these colonies may be derived from preleukemic, non-*FLT3*–mutant HPSCs[4,6] or from normal progenitors.

Genomic interrogation of patients who relapsed on quizartinib reveals on- and off-target mutations

We sought to examine both *FLT3*-dependent and -independent mechanisms of resistance in a larger cohort of clinical patient samples. In total, we subjected the *FLT3* KD (of both ITD$^+$ and native *FLT3* alleles) of 15 patients with acquired resistance to quizartinib to single-molecule real-time sequencing, direct sequencing, or PCR amplification and subcloning, including 8 patients reported in our previous analysis.[13] We detected *FLT3* KD mutations in 14 of 15 samples (Table 2). To identify putative mechanisms of off-target resistance, we performed targeted next-generation sequencing of mutation hotspots

Figure 2. Genetic heterogeneity revealed by single-cell sorting of samples from patients relapsed on quizartinib. (A) Schematic of experimental setup for single-cell sorting followed by *FLT3* mutation genotyping. Percent of cells with indicated *FLT3* genotype in patients (B) 1005-007, (C) 1005-009, and (D) 1009-003. Each circle represents a particular *FLT3* genotype. The relative size of circles is representative of the relative proportion of the overall population with that genotype.

Table 2. *FLT3* KD mutations found at relapse in patients with bone marrow responses on quizartinib

Patients number	Sex	Age (y)	Prior therapy	Karyotype pretreatment	Karyotype at relapse	Bone marrow blasts in relapse sample (%)	Quizartinib dose (mg)	Bone marrow blasts at best response (%)	*FLT3* KD mutation at relapse	Mutation detection method	Weeks on study
1009-003	F	75	7+3	45~54,XX,+3,+6,+7,+8,+13,+14, +21,+22[cp15]/46,XX[5]	52,XX,+3,+6,+7,+8,+10,+12,+ 13[cp7]/46,XX[14]	90	90, increased to 135 for refractory disease	<5	D835F, D835Y, D835V	SMRT sequencing	12
1009-007	F	64	7+3, HiDAC	Normal	ND	75	90, reduced to 60 for QT prolongation	<5	D835Y	SMRT sequencing	10
1009-014	M	62	7+3, HAM	Normal	ND	10-15	135, reduced to 90 for QT prolongation	<5	D835V	PCR subcloning	10
1009-018	M	70	7+3, HiDAC	45,X,-Y,add(2)(p12),t(6;19)(p21; q11.2),t(8;21)(q22;q22),add(16)(q13), add(20)(q?13.1)[20]	45,X,-Y, add(2)(p12), t(6;19)(p21;q11.2), t(8;21)(q22;q22), add(16)(q13), add(20)(q?13.1)[3]/46, XY[2]	38	135, reduced to 90 for QT prolongation	<5	None	PCR subcloning	15
1009-019	M	52	7+3, HiDAC, Cytoxan/TBI	46, XY, add(6)(p21),del(8)(p21), add(12)(q24.1)[13]/46,XY,del(1)(q32), del(7)(q22q32),der(6;12)(q10;p10), add(22)(q?11.2),+mar[3]/45,XY, t(1;2)(p?22;q11.2)-21[1]/46,XY[3]	ND	68	135	<5	D835Y	PCR subcloning	10
1009-021	M	65	Azacitidine + sapacitabine	46,XY,+11[15]	46,XY,+11[13]/47,sl,add(17) (p11.2)[9]	45	135	10	D835Y	PCR subcloning	18
3351-1085	F	69	Clofarabine, MEC	Normal	No growth, most recent karyotype during response: 46,XX,t(8;12)(q12; p13),add(10)(q11,2),-11,+mar[5]/46, XX[15]	78	30, increased to 60 for refractory disease	<5	D835Y	PCR subcloning	11
1011-006	M	70	7+3, low-dose cytarabine	Normal	ND	10	200	5	D835Y	SMRT sequencing	7
1011-007	F	56	7+3, HAM	Normal	46,XX,del(11)(p?13p?15)[12]/46, XX[9]	80	200	<5	F691L, D835V, D835Y	SMRT sequencing	8
1005-004	F	60	Cytarabine and mitoxantrone	Normal	Normal	92	200	<5	F691L	SMRT sequencing	19
1005-006	M	43	7+3, MEC	46,XY,t(1;15)(p22;q15)	ND	59	200	<5	D835Y, D835F	SMRT sequencing	6
1005-007	F	59	7+3, HiDAC	Normal	ND	39	135	<5	D835V, D835Y	SMRT sequencing	23
1005-009	M	68	Cytarabine and mitoxantrone	Normal	ND	58	135	<5	D835Y	SMRT sequencing	18
1005-010	M	52	7+3, HiDAC, mitoxantrone, and etoposide	46,XY,t(4;12)(q26;p11.2), t(8;14)(q13;q11.2)	ND	22	135	<5	F691L	SMRT sequencing	19
512-92-61 (0820-1039)	F	64	7+3, carboplatin and topotecan	Normal	46,XX,t(5;7)(q15;p15)[2]/46,XX[18]	80	30, increased to 60 for refractory disease	<5	D835I	PCR subcloning	8
1009-011*	F	33	7+3, HiDAC, G-CLAC	Normal	NA	<5	90	<5	NA	NA	Off study for transplant after 6 weeks

F, female; G-CLAC, G-CSF clofarabine high-dose cytarabine (Ara-C); HAM, high-dose Ara-C mitoxantrone; HiDAC, high-dose Ara-C; M, male; MEC, mitoxantrone etoposide cytarabine (Ara-C); NA, not applicable; ND, not done; QT, QT interval; SMRT, single-molecule real-time [sequencing]; TBI, total body irradiation.

*Patient did not relapse on study drug; no relapse sample sequenced.

from a panel of 33 AML-relevant genes (supplemental Table 7)[25] in relapse and pretreatment DNA from 4 patients (1005-007, 1005-009, 1009-003, and 3351-1085) noted in this study to exhibit both *FLT3*-dependent and suspected *FLT3*-independent resistance. We sequenced to 3000X depth and identified mutations in genes other than *FLT3* in pretreatment samples from 3 of 4 patients (supplemental Table 8). However, we detected no new mutations other than the previously identified relapse-associated *FLT3* KD mutations at the time of disease relapse (data not shown). Of these patients, it is notable that one patient (3351-1085) had evidence of clonal evolution with new cytogenetic abnormalities detected during drug response (Table 2), although a karyotype was not obtained at the time of relapse. In the remaining patients, 1009-003 had no evidence of clonal evolution by cytogenetics and 2 others (1005-007 and 1005-009) had no karyotype analysis performed at the time of relapse.

To expand our investigation to genes not previously associated with AML, we performed whole-exome sequencing of paired pretreatment and relapse samples from 3 of these 4 patients (1005-007, 1009-003, and 3351-1085) from whom sufficient DNA was available. By sequencing to a depth of ~100X, we identified a small number of coding mutations (3 to 7 per patient) that were acquired at the time of TKI resistance (supplemental Table 9). None of the identified mutations were recognized in more than 1 patient or had been previously associated with AML or TKI resistance. The acquisition of new mutations at the time of relapse in quizartinib-resistant patients is indicative of clonal evolution at the time of disease progression. However, functional studies will be required to definitively verify which, if any, of these mutations drive clinical resistance or whether these mutations serve as passengers without a true role in drug resistance.

Discussion

Genomic studies in solid tumors have revealed significant branching intratumoral clonal genetic heterogeneity,[30,31] including a recent study that identified as many as 5 driver mutations in a single melanoma patient at the time of relapse on the targeted *BRAF* inhibitor dabrafenib.[31] Such complexity is not surprising in solid tumors, particularly melanoma, where ultraviolet (UV)-induced DNA damage creates one of the highest mutational burdens observed in human malignancies. Here, we demonstrate that even in AML, one of the most genetically simple of all adult malignancies with an average of only 13 coding mutations and 3 or fewer clones identified per tumor,[1] considerable genetic heterogeneity undermines response to the targeted therapeutic quizartinib. Although *FLT3*-dependent resistance seemed to develop in the majority of patients (14 of 15) examined and included drug-resistant *FLT3* D835 mutations occurring on both ITD- and native *FLT3*-containing alleles, single-cell analysis of the *FLT3* locus revealed a high degree of mutational heterogeneity within *FLT3* and suggested that coexisting off-target resistance mechanisms may be more prominent than previously appreciated. It is striking that interrogation of this single tumor-relevant locus revealed such complexity and it seems likely that single-cell interrogation of other genetic loci would add exponentially to the degree of tumor heterogeneity observed. Regardless, the common finding of polyclonal resistance mechanisms argues strongly that targeted mono- and even dual-therapy strategies in AML are unlikely to achieve durable responses in the vast majority of patients. Although a substantial reduction in disease bulk may be achieved with a single targeted therapeutic and on-target resistance mechanisms may be potentially addressed by a combination of TKIs with nonoverlapping mutational resistance profiles, as we have previously suggested,[32,33] a better understanding of off-target mechanisms of resistance coupled with the incorporation of agents that can override these off-target mechanisms will be essential to substantially improving therapeutic outcomes.

Recent studies have confirmed that activating mutations in *FLT3* occur relatively late in leukemogenesis[4,6] and can represent a marker for the transition of preleukemic to leukemic stem cells. They suggest that under the selective pressure of an FLT3 inhibitor, a preleukemic stem cell may easily evolve into a non-FLT3–dependent subclone. Consistent with this possibility, *FLT3* mutations have been noted to be lost (or become undetectable) at disease relapse after chemotherapy.[34] Remarkably, in the majority of patients in our study, a large proportion of the bulk tumor population remained dependent on late-occurring *FLT3* mutations, as evidenced by the fact that the majority of patients evolved a drug-resistant *FLT3* KD mutation at disease relapse, most at the D835 residue, and that several patients evolved more than 1 mutation, on both ITD-containing and native *FLT3* alleles.

The observation of convergent D835 mutations occurring on both ITD^+ and native *FLT3* alleles at the time of resistance can be explained by 2 models. In the first model, resistance evolves from both ancestral *FLT3-ITD*$^+$ and *FLT3* native clones, which suggests branching tumor evolution under the selection of FLT3 inhibitor therapy (Figure 4A) and implies that some *FLT3* native clones can also be dependent on FLT3 signaling. In the second model, multiple *FLT3* mutational events occur in separate HPSCs in parallel to give rise to polyclonal leukemic blast populations that are later enriched for cells containing D835 mutations on quizartinib therapy (Figure 4B). Regardless of which models are operative, our findings provide compelling evidence for complex evolution of these resistance-conferring mutations. These data also reinforce the central advantage that *FLT3* mutations confer in the process of leukemogenesis. However, the concomitant presence of a significant proportion of cells with presumed off-target resistance (cells containing *FLT3*-ITD without KD mutations) in all patients interrogated at this level suggests that bypass of reliance upon FLT3 activity may occur, although it is also possible that uncharacterized epigenetic or drug efflux mechanisms may also play a role. In aggregate, these data confirm that polyclonal resistance mechanisms commonly coexist in individual patients. Importantly, although recent genomic sequencing efforts have elucidated the genetic landscape of de novo AML, whole-exome sequencing in our study reveals that clonal evolution of mutations occurs in genes not previously associated with AML at the time of relapse on quizartinib. These data imply that the scope of mutations and intratumoral heterogeneity observed after relapse on chemotherapy may differ significantly from that observed in de novo disease, because of either selection for previously undetected chemotherapy-resistant clones or the mutagenic effects of therapy itself.

Ultimately, combination strategies that can address both on- and off-target resistance and are capable of eradicating chemotherapy-resistant preleukemic stem cells will be required to effect durable therapeutic responses. To this end, incorporation of therapies targeting gene expression, such as DNA methyltransferase inhibitors[35] has already been explored in concert with FLT3 inhibitors, and these therapies have been noted to be clinically active. Preclinical studies have implicated the chromatin reader BRD4 as an important regulator of transcriptional

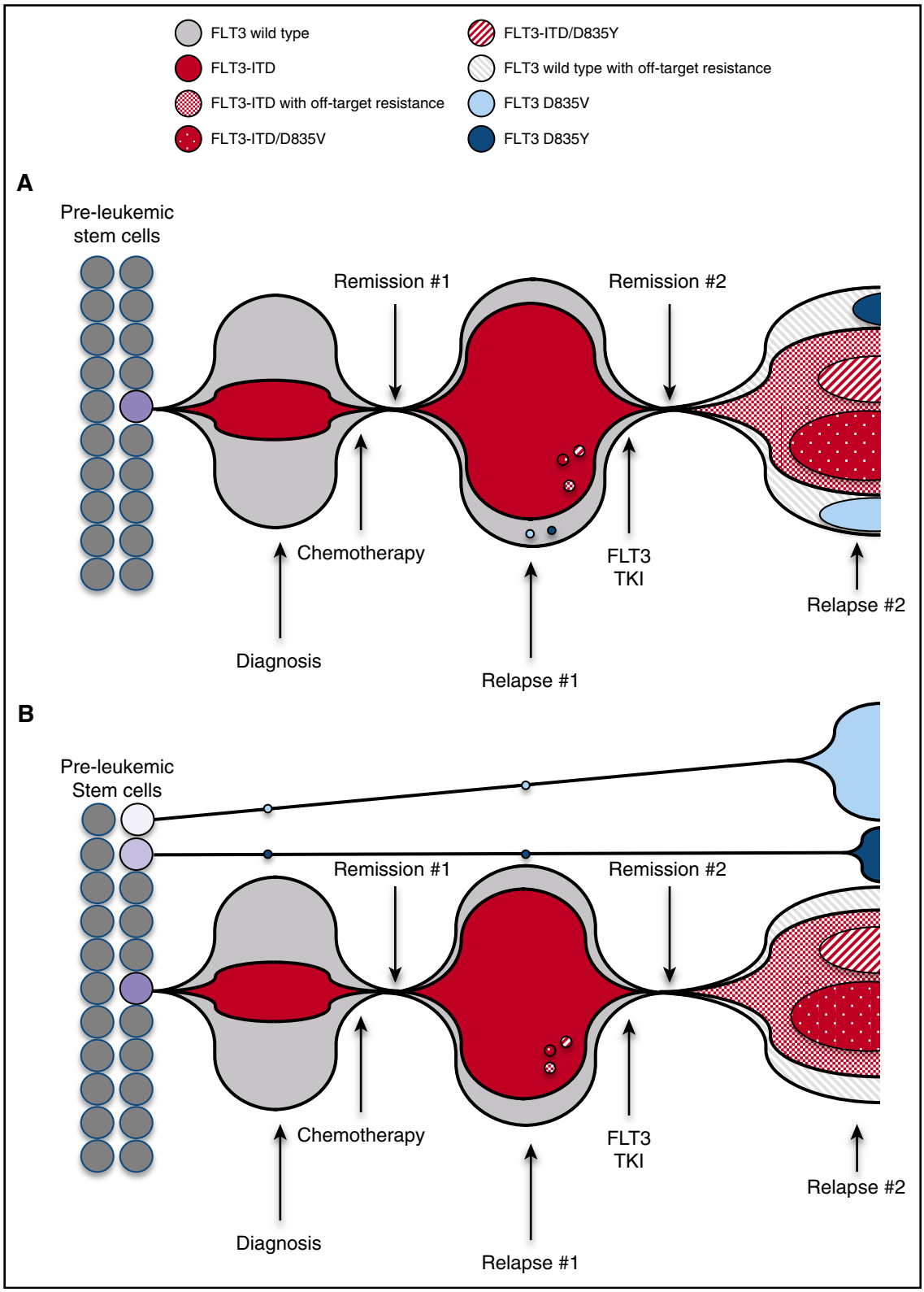

Figure 4. Models for evolution of polyclonal FLT3-dependent and non-FLT3–dependent resistance after TKI treatment. Schematic representation illustrates proportion of *FLT3* mutant and native *FLT3* leukemia cell population at treatment time points. (A) At diagnosis, *FLT3*-ITD$^+$ cells represent a portion of bulk tumor. Debulking after chemotherapy results in Remission #1, but is followed by emergence of chemotherapy-resistant FLT3-dependent leukemia cell populations at the time of Relapse #1. FLT3 TKI treatment induces Remission #2, but at the time of Relapse #2, multiple drug-resistant clones evolve, including *FLT3* cells containing ITD and native *FLT3* cells. (B) At diagnosis, *FLT3*-ITD$^+$ cells represent a portion of bulk tumor. *FLT3* D835V and D835Y mutations arise on native *FLT3* alleles in separate leukemic stem cells, and these clones persist through chemotherapy. Debulking after chemotherapy results in Remission #1 but is followed by the emergence of chemotherapy-resistant FLT3-dependent leukemia cell populations at the time of Relapse #1. FLT3 TKI treatment induces Remission #2, but at the time of Relapse #2, multiple drug-resistant clones arise, including *FLT3*-ITD–containing clones (D835-mutant and off-target resistant), expansion of TKI-resistant native *FLT3* D835–mutant clones, and off-target–resistant native *FLT3* clones.

activation in AML.[36] Preclinical[37,38] and early clinical[39] studies of small molecule BRD4 inhibitors have demonstrated activity in a variety of AML subtypes and may also represent a potentially efficacious partner for targeting leukemic stem cells. Other compounds aimed at targeting epigenetic deregulation in AML have entered or are poised to enter clinical trials, including inhibitors of the histone demethylase LSD1 and the lysine methyltransferase DOT1L,[40] and they provide additional candidates for combination therapy. In the future, immunotherapy approaches such as chimeric antigen receptor–modified T cells targeting AML stem and progenitor cell antigens may provide additional therapeutic opportunities for use with FLT3 inhibitors, although identification of appropriate antigens currently remains challenging.

Acknowledgments

This work was supported in part by grants 1RO1 CA176091 (N.P.S.), 5P30CA82103 (A.O.), K08 CA187577 (C.C.S.), R01 CA149566 (A.P. and J.P.R.), R01 CA1752515 (A.P. and J.P.R.), and R01 CA175008 (A.P., and J.P.R.), and Specialized Programs of Research Excellence grant P50 CA100632 (M.J.L.) from the National Institutes of Health, National Cancer Institute, and by the Edward S. Ageno Foundation (N.P.S.). C.C.S. is an American Society of Hematology faculty scholar and recipient of a Hellman Family Foundation Early Career Faculty Award.

Authorship

Contribution: C.C.S. and A.P. designed experiments, performed research, and wrote the manuscript; M.J.L., A.E.P., J.P.R., and N.P.S. designed experiments, supervised research, and wrote the manuscript; G.R.J., K.C.L., T.T., K.J.T., E.M., and S.W. performed experiments; and C.-S.C., S.A., and A.O. provided bioinformatics data analysis.

Conflict-of-interest disclosure: N.P.S. received research funding for conducting clinical trials from ARIAD Pharmaceuticals and Ambit Biosciences and research funding from Daiichi-Sankyo and Plexxikon, Inc. C.C.S. received research funding from Plexxikon, Inc. and Astellas Pharma. A.P. consulted for Daiichi Sankyo, Astellas Pharma, Novartis, Pfizer, Asana Biosciences, and Arog Pharmaceuticals. M.J.L. consulted for Daiichi-Sankyo, Astellas Pharma, Novartis, and Arog Pharmaceuticals. K.J.T., S.W., and C.-S.C. hold stock in Pacific Biosciences. The remaining authors declare no competing financial interests.

The current affiliation for K.J.T. is Roche Sequencing Solutions, Santa Clara, CA.

The current affiliation for S.W. is 10X Genomics, San Francisco, CA.

ORCID profiles: C.C.S., 0000-0003-0160-7026; A.P., 0000-0002-6819-9736; G.R.J., 0000-0001-6271-7750; T.T., 0000-0002-2058-7609; C.-S.C., 0000-0003-4394-2455; J.P.R., 0000-0002-1618-230X.

Correspondence: Neil P. Shah, 505 Parnassus Ave, Suite M1286, Box 1270, San Francisco, CA 94143; e-mail: nshah@medicine.ucsf.edu.

References

1. Cancer Genome Atlas Research Network. Genomic and epigenomic landscapes of adult de novo acute myeloid leukemia. *N Engl J Med*. 2013;368(22):2059-2074.
2. Patel JP, Gönen M, Figueroa ME, et al. Prognostic relevance of integrated genetic profiling in acute myeloid leukemia. *N Engl J Med*. 2012;366(12):1079-1089.
3. Welch JS, Ley TJ, Link DC, et al. The origin and evolution of mutations in acute myeloid leukemia. *Cell*. 2012;150(2):264-278.
4. Jan M, Snyder TM, Corces-Zimmerman MR, et al. Clonal evolution of preleukemic hematopoietic stem cells precedes human acute myeloid leukemia. *Sci Transl Med*. 2012;4(149):149ra118.
5. Shlush LI, Zandi S, Mitchell A, et al; HALT Pan-Leukemia Gene Panel Consortium. Identification of pre-leukaemic haematopoietic stem cells in acute leukaemia. *Nature*. 2014;506(7488):328-333.
6. Corces-Zimmerman MR, Hong WJ, Weissman IL, Medeiros BC, Majeti R. Preleukemic mutations in human acute myeloid leukemia affect epigenetic regulators and persist in remission. *Proc Natl Acad Sci USA*. 2014;111(7):2548-2553.
7. Paguirigan AL, Smith J, Meshinchi S, Carroll M, Maley C, Radich JP. Single-cell genotyping demonstrates complex clonal diversity in acute myeloid leukemia. *Sci Transl Med*. 2015;7(281):281re2.
8. Ding L, Ley TJ, Larson DE, et al. Clonal evolution in relapsed acute myeloid leukaemia revealed by whole-genome sequencing. *Nature*. 2012;481(7382):506-510.
9. Klco JM, Spencer DH, Miller CA, et al. Functional heterogeneity of genetically defined subclones in acute myeloid leukemia. *Cancer Cell*. 2014;25(3):379-392.
10. Tallman MS, Schiller G, Trone D, et al. Results of a phase 2 randomized, open-label, study of lower doses of quizartinib (AC220; ASP2689) in subjects with FLT3-ITD positive relapsed or refractory acute myeloid leukemia (AML) [abstract]. *Blood*. 2013;122(21). Abstract 494.
11. Levis MJ, Perl AE, Dombret H, et al. Final results of a phase 2 open-label, monotherapy efficacy and safety study of quizartinib (AC220) in patients with FLT3-ITD positive or negative relapsed/refractory acute myeloid leukemia after second-line chemotherapy or hematopoietic stem cell transplantation [abstract]. *Blood*. 2012;120(21). Abstract 673.
12. Cortes JE, Perl AE, Dombret H, et al. Final results of a phase 2 open-label, monotherapy efficacy and safety study of quizartinib (AC220) in patients ≥ 60 years of age with FLT3 ITD positive or negative relapsed/refractory acute myeloid leukemia [abstract]. *Blood*. 2012;120(21). Abstract 48.
13. Smith CC, Wang Q, Chin CS, et al. Validation of ITD mutations in FLT3 as a therapeutic target in human acute myeloid leukaemia. *Nature*. 2012;485(7397):260-263.
14. Albers C, Leischner H, Verbeek M, et al. The secondary FLT3-ITD F691L mutation induces resistance to AC220 in FLT3-ITD+ AML but retains in vitro sensitivity to PKC412 and Sunitinib. *Leukemia*. 2013;27(6):1416-1418.
15. Baker SD, Zimmerman EI, Wang YD, et al. Emergence of polyclonal FLT3 tyrosine kinase domain mutations during sequential therapy with sorafenib and sunitinib in FLT3-ITD-positive acute myeloid leukemia. *Clin Cancer Res*. 2013;19(20):5758-5768.
16. Man CH, Fung TK, Ho C, et al. Sorafenib treatment of FLT3-ITD(+) acute myeloid leukemia: favorable initial outcome and mechanisms of subsequent nonresponsiveness associated with the emergence of a D835 mutation. *Blood*. 2012;119(22):5133-5143.
17. Metzelder SK, Schroeder T, Finck A, et al. High activity of sorafenib in FLT3-ITD-positive acute myeloid leukemia synergizes with allo-immune effects to induce sustained responses. *Leukemia*. 2012;26(11):2353-2359.
18. Woyach JA, Furman RR, Liu TM, et al. Resistance mechanisms for the Bruton's tyrosine kinase inhibitor ibrutinib. *N Engl J Med*. 2014;370(24):2286-2294.
19. Nazarian R, Shi H, Wang Q, et al. Melanomas acquire resistance to B-RAF(V600E) inhibition by RTK or N-RAS upregulation. *Nature*. 2010;468(7326):973-977.
20. Johannessen CM, Boehm JS, Kim SY, et al. COT drives resistance to RAF inhibition through MAP kinase pathway reactivation. *Nature*. 2010;468(7326):968-972.
21. Emery CM, Vijayendran KG, Zipser MC, et al. MEK1 mutations confer resistance to MEK and B-RAF inhibition. *Proc Natl Acad Sci USA*. 2009;106(48):20411-20416.
22. Engelman JA, Zejnullahu K, Mitsudomi T, et al. MET amplification leads to gefitinib resistance in lung cancer by activating ERBB3 signaling. *Science*. 2007;316(5827):1039-1043.
23. Smith CC, Lasater EA, Zhu X, et al. Activity of ponatinib against clinically-relevant AC220-resistant kinase domain mutants of FLT3-ITD. *Blood*. 2013;121(16):3165-3171.
24. Thompson JE, Conlon JP, Yang X, Sanchez PV, Carroll M. Enhanced growth of myelodysplastic colonies in hypoxic conditions. *Exp Hematol*. 2007;35(1):21-31.
25. Sehgal AR, Gimotty PA, Zhao J, et al. DNMT3A mutational status affects the results of dose-escalated induction therapy in acute myelogenous leukemia. *Clin Cancer Res*. 2015;21(7):1614-1620.
26. Li H, Durbin R. Fast and accurate short read alignment with Burrows-Wheeler transform. *Bioinformatics*. 2009;25(14):1754-1760.

27. McKenna A, Hanna M, Banks E, et al. The Genome Analysis Toolkit: a MapReduce framework for analyzing next-generation DNA sequencing data. *Genome Res*. 2010;20(9): 1297-1303.

28. Cibulskis K, Lawrence MS, Carter SL, et al. Sensitive detection of somatic point mutations in impure and heterogeneous cancer samples. *Nat Biotechnol*. 2013;31(3):213-219.

29. Yamamoto Y, Kiyoi H, Nakano Y, et al. Activating mutation of D835 within the activation loop of FLT3 in human hematologic malignancies. *Blood*. 2001;97(8):2434-2439.

30. Gerlinger M, Rowan AJ, Horswell S, et al. Intratumor heterogeneity and branched evolution revealed by multiregion sequencing. *N Engl J Med*. 2012;366(10):883-892.

31. Shi H, Hugo W, Kong X, et al. Acquired resistance and clonal evolution in melanoma during BRAF inhibitor therapy. *Cancer Discov*. 2014;4(1):80-93.

32. Smith CC, Lasater EA, Lin KC, et al. Crenolanib is a selective type I pan-FLT3 inhibitor. *Proc Natl Acad Sci USA*. 2014;111(14):5319-5324.

33. Smith CC, Zhang C, Lin KC, et al. Characterizing and overriding the structural mechanism of the quizartinib-resistant FLT3 "gatekeeper" F691L mutation with PLX3397. *Cancer Discov*. 2015; 5(6):668-679.

34. Kottaridis PD, Gale RE, Langabeer SE, Frew ME, Bowen DT, Linch DC. Studies of FLT3 mutations in paired presentation and relapse samples from patients with acute myeloid leukemia: implications for the role of FLT3 mutations in leukemogenesis, minimal residual disease detection, and possible therapy with FLT3 inhibitors. *Blood*. 2002;100(7): 2393-2398.

35. Ravandi F, Alattar ML, Grunwald MR, et al. Phase 2 study of azacytidine plus sorafenib in patients with acute myeloid leukemia and FLT-3 internal tandem duplication mutation. *Blood*. 2013;121(23):4655-4662.

36. Roe JS, Mercan F, Rivera K, Pappin DJ, Vakoc CR. BET bromodomain inhibition suppresses the function of hematopoietic transcription factors in acute myeloid leukemia. *Mol Cell*. 2015;58(6): 1028-1039.

37. Dawson MA, Prinjha RK, Dittmann A, et al. Inhibition of BET recruitment to chromatin as an effective treatment for MLL-fusion leukaemia. *Nature*. 2011;478(7370):529-533.

38. Zuber J, Shi J, Wang E, et al. RNAi screen identifies Brd4 as a therapeutic target in acute myeloid leukaemia. *Nature*. 2011;478(7370):524-528.

39. Berthon C, Raffoux E, Thomas X, et al. Bromodomain inhibitor OTX015 in patients with acute leukaemia: a dose-escalation, phase 1 study. *Lancet Haematol*. 2016;3(4): e186-e195.

40. Wouters BJ, Delwel R. Epigenetics and approaches to targeted epigenetic therapy in acute myeloid leukemia. *Blood*. 2016;127(1):42-52.